Main Injector Gap Clearing Kicker Design Review
Chris Jensen, 10/3/08
Field simulations by Iouri Terechkine

0 Background

The kicker system requirements were originally conceived for the NOvA project. NOvA is a neutrino experiment located in Minnesota. To achieve the desired neutrino flux several upgrades are required to the accelerator complex. The Recycler will be used as a proton pre-injector for the Main Injector (MI). As the Recycler is the same size as the MI, it is possible to do a single turn fill (~11 μsec), minimizing the proton injection time in the MI cycle and maximizing the protons on target. The Recycler can then be filled with beam while the MI is ramping to extract beam to the target. To do this requires two new transfer lines. The existing Recycler injection line was designed for 10π pbar beams, not the 20π proton beams we anticipate from the Booster. The existing Recycler extraction line allows for proton injection through the MI, while we want direct injection from the Booster. These two lines will be decommissioned. The new injection line from the MI8 line into the Recycler will start at 848 and end with injection kickers at RR104. The new extraction line in the RR30 straight section will start with a new extraction kicker at RR232 and end with new MI injection kickers at MI308. Finally, to reduce beam loss activation in the enclosure, a new gap clearing kicker will be used to extract uncaptured beam created during the slip stack injection process down the existing dump line. It was suggested that the MI could benefit from this type of system immediately. This led to the early installation of the gap clearing system in the MI, followed by moving the system to Recycler during NOvA.

The specifications also changed during this process. Initially the rise and fall time requirements were 38 ns and the field stability was ±1%. The 38 ns is based on having a gap of 2 RF buckets between injections. (There are 84 RF buckets that can be filled from the Booster for each injection, but 82 would be filled with beam. MI and Recycler contain 588 RF buckets.) A rough cost / benefit analysis showed that increasing the number of empty buckets to 3 decreased the kicker system cost by ~30%. This could be done while not extending the running time since this is only a 1% reduction in protons per pulse, hence the rise and fall time are now 57 ns. Additionally, the ±1% tolerance would have required a fast correction kicker while ±3% could be achieved without this kicker. The loosened tolerance was based on experience on wide band damping systems in the MI. A higher power wideband damping system is a better use of the resources as it can be used to correct for multiple sources of emittance growth. Finally, with the use of this system for MI instead of Recycler, the required strength grew from 1.2 mrad to 1.7 mrad. The final requirements for this kicker are listed below.

Angle	1.70 mrad, horizontal, to outside of ring for MI Gap Clearing
	1.21 mrad, horizontal, to outside of ring for RR Injection
	1.18 mrad, horizontal, to outside, for RR Gap Clearing
Field Rise Time	57 ns
Field Fall Time	57 ns for RR Injection and RR Gap Clearing
Field Fall Time	<400 ns for MI Gap Clearing (Meas fall time of MI Injection kicker)
Flattop stability	±3%
Pre and Post Stability	±3%

1 Initial System Design

The MI Gap Clearing kicker system will be built on the model of previous fast kicker magnets; the MI injection kicker and Booster extraction kicker. It will have a magnetic aperture of 53 mm x 110 mm (to meet the beam aperture of 33 mm x 81 mm). We will use the same magnet to meet all three requirements. Experience has shown that building and testing a prototype magnet is required when new designs are done and each new magnet design requires a minimum 2 years of effort. Measurements are required to complete design choices and minor changes may be required to meet the specification.

The magnets for the kicker must be transmission line style. They will be terminated with the characteristic impedance to give a flat pulse shape. Given an achievable pulser voltage rise time (3% to 97%) of < 25 ns the magnet fill time must be less than 32 ns. Typical end effects for each magnet (vacuum fitting, high voltage input and output) are about 12" per end. Given the fill time required, the only reasonable choice of Z0 is 50 ohms. The high voltage cable we use is 50 ohms and lower impedance of two cables in parallel would make ineffective use of beam line space, i.e. the ratio of magnetic length to physical length would be low.

Because the system will be running at a variety of average repetition rates, the effect of average power on the magnet termination resistance has to be no more than ~1%. This has been done successfully on previous systems. The main pulser will be a coaxial cable pulse forming line (PFL) with a thyratron switch. The cable will be pulse charged so that the thyratron can be run at high reservoir, and therefore high speed, while minimizing pre-fires. Two variations of cable are available from Times, AA 5967 and a larger AA 8740. Dispersive losses in a cable lead to a longer fall time than rise time and higher droop. The larger AA 8740 cable has about 2/3 the losses so it will be used. Ferrite pulse sharpening (saturating ferrite cores placed at the output lead of the thyratron) will also be incorporated. We have done preliminary testing on a slightly modified version of a previous pulser to confirm that we can get a faster rise time with the use of saturating ferrite cores. Finally, the main pulser is passive on the falling edge, so the fall time will be longer than the rise time due to dispersion in the cable. This is not an issue for MI Gap Clearing but is for NOvA. The main pulser design is not covered further in this document.

When the system is used for NOvA it is expected to need a "bumper" system to cancel the tail and allow the system to meet the fall time requirement to the 3% level. The system will consist of a pulsed power supply driving an additional kicker magnet in the tunnel. The general requirements for the bumper power supply are known from existing measurements. The bumper system will consist of a pulse forming network (PFN) with a few sections and use the same thyratron as the main system. It will use the same magnet as the main kick. The stray inductance and capacitance are different for thyratron anode and cathode and so cause a change in waveform when reversed. Therefore, so that the thyratron does not change orientation, the bumper magnet orientation will be upside down and backwards. This is another constraint on the magnet design. This orientation also maintains the largest possible kick strength as the magnetic kick and electric kick will add.

With these design parameters, the magnetic length is limited to ~0.7 meters. Each magnet will have a nominal angle (for 8GeV protons) of 270 μrad at the nominal current of 450 A and a maximum current of 550 A. The 550 A limit is actually the 55 kV maximum voltage limit on the pulse forming line and on fast thyratrons. We get long lifetime on pulse forming lines (Times Microwave AA 5966) when the operating voltage is under 55 kV and two gap thyratrons are limited to about 55 kV DC charge voltage. In order to get the kick required for MI gap clearing,

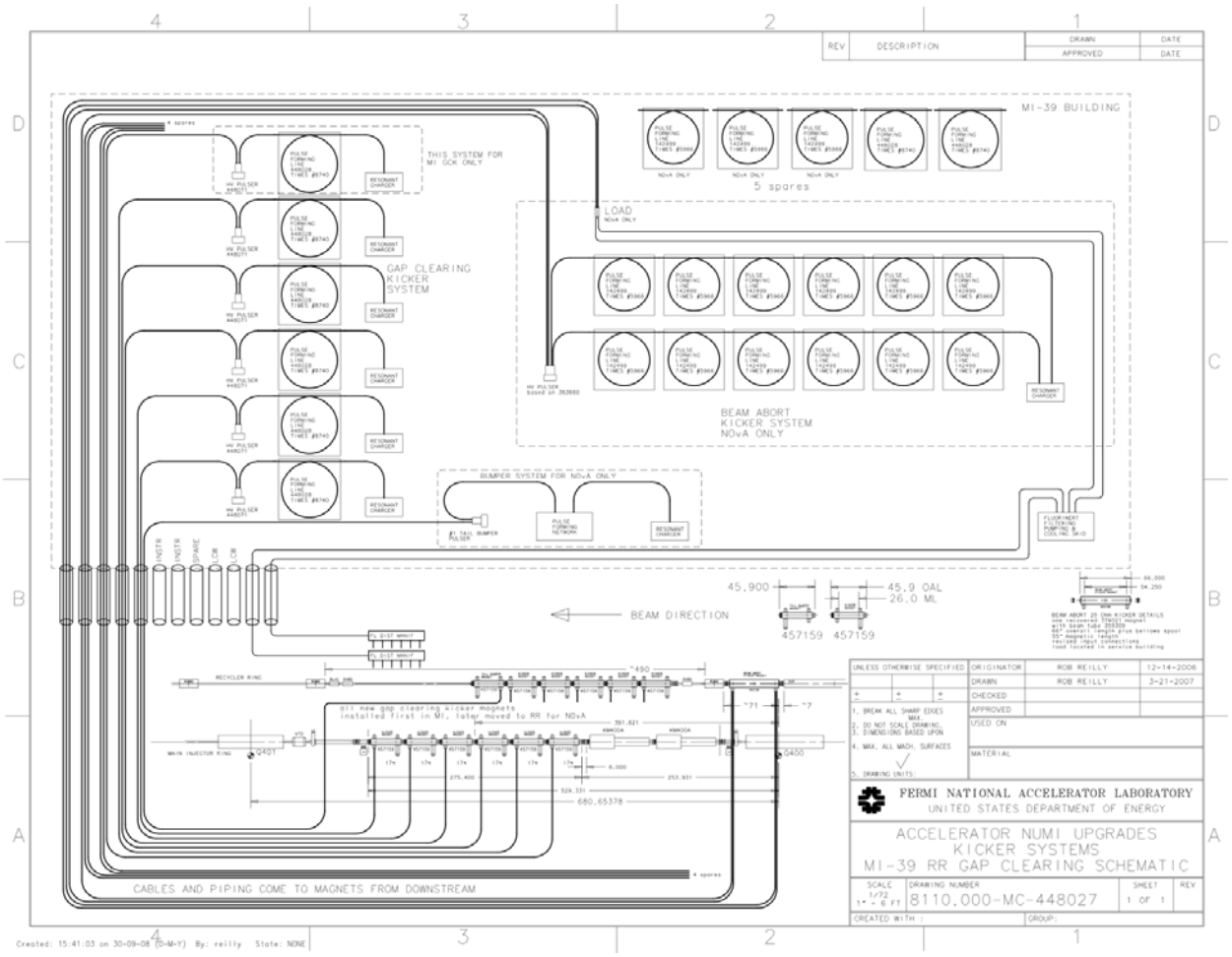

The 6 magnet system might have limited tuning range for MI operation, but this operation should last for only a couple years. There is ample tuning range for Recycler operation where only 5 magnets will be used for the main kick and one for the bumper. A proposed layout, including cabling, penetrations from the MI 39 service building, and cooling piping is shown in Figure 1.

2 Detailed Magnet Design

Several fast kicker magnets have been built over the years. Existing designs and their rough capabilities are shown in Table 1. The MI injection kicker magnet design is over 10 years old and Booster kicker magnet is over 20 years old. Some modification based on more recent magnets can be applied to these to improve response.

Magnet Type	Electrical Impedance	Total Inductance	Propagation Time	Field Rise	Nominal Field	Magnetic Gap x Electric Gap (cm)	Magnetic Length (m)
Booster Kicker	50 Ohm	1250 nH	27 ns	~ 35ns	10 mT	7.3 cm x 7.0 cm	1.08 m
MI Injection	25 Ohm	710 nH	28 ns	~ 50 ns	6.8 mT	11.1 cm x 6.3 cm	0.79 m
MIGCK (NEW)	50 Ohm	1600 nH	32 ns	57 ns	11.3 mT	5.3 cm x 11.0 cm	0.7 m

Table 1 Comparing Existing Magnet Parameter to New Design.

Both the MI and Booster kicker magnets are potted with room temperature vulcanizing (RTV) silicon rubber. Liquid (insulating oil) filling of magnet makes repair of the magnet possible. However, the main problem to date with that style of magnet has been leaking liquid. The possibility of liquid filling of the magnet will be kept as a backup plan and designed into the magnet.

There are several criteria in deciding the number of sections in the magnet. One primary one is the expected rise time of the magnet. The rise time for a matched traveling wave magnet has approximately same time as one time constant of inductive load. The fill time however depends upon the amount of segmentation in the magnet and the rise time of the pulser driving the magnet. The design can only work when the magnet also has a damped response to pulses with a fast rise time. So, for a magnetic field rise time of less than 57 ns, we can calculate the minimum number of cells for a given impedance, rise time, inductance and for several rise time definitions. The basic equation is:

$\tau_{field\ rise} = \tau_{volt\ fill} + \tau_{volt\ rise}$

where $\tau_{volt\ fill}$ is the time for the wave to propagate through the magnet $\tau_{volt\ rise}$ is the voltage rise time at the magnet output. The voltage rise time will degrade as it propagates through the magnet due to losses and section to section coupling, both lead to dispersion. The field rise time can then be expressed roughly as follows:

$\tau_{field\ rise}$ (2-98%)= $N\sqrt{L\,C}$ + MAX [$\tau_{volt\ rise}$, ~$30\sqrt{L\,C}$]

$\tau_{field\ rise}$ (5-95%)= $N\sqrt{L\,C}$ + MAX [$\tau_{volt\ rise}$, ~$20\sqrt{L\,C}$]

where

N is the number of sections in the magnet
L is the inductance per section
C is the capacitance per section
Factor 20 or 30 is based on numerical simulations from previous magnet designs

We can perform some manipulations if we first estimate that input voltage rise time is less than the magnet output voltage rise time. Then using the relationships:

$$Z_0 = \sqrt{\frac{L}{C}} \qquad \text{where } L_{magnet} = N\,L \qquad \text{and } C_{magnet} = N\,C$$

we have for the 2 - 98% rise time

$$\tau_{field\ rise} = \sqrt{L_{magnet}\ C_{magnet}} + \sim\frac{30}{N}\sqrt{L_{magnet}\,C_{magnet}}$$

$$= \sqrt{L_{magnet}\ \frac{L_{magnet}}{Z_0^2}} + \frac{30}{N}\sqrt{L_{magnet}\ \frac{L_{magnet}}{Z_0^2}}$$

$$= \left[\,1 + \frac{30}{N}\,\right]\frac{L_{magnet}}{Z_0} \Rightarrow$$

$$N(2\text{-}98\%) \sim \frac{30}{\left[\,\frac{Z_0\,\tau_{field\ rise}}{L_{magnet}} - 1\,\right]} = \frac{30}{\left[\frac{50\Omega(57ns)}{1600nH} 1\right]} = 38 \text{ sections}$$

Similarly for the 5-95% rise time, N(2-98%) ~ 25 sections. There is a fairly strong dependence on the number of sections given the rise time definition. If we assume we have very little dispersion in the magnet, then the number of sections is a free choice. Since we have a range, we will start with 32 sections and then do a circuit simulation to verify these estimates. The actual capacitance required should also be calculated to make sure it is reasonable.

$$C = \frac{1600nH}{(50Ohm)^2} = 640 \text{ pF}, \quad C/m = \frac{640pF}{0.7m} = 914 \text{ pF/m}, \quad C/sec = \frac{640pF}{32} = 20 \text{ pF}$$

Because the required capacitance is relatively small, the new kicker magnet will use geometry to achieve the required capacitance (in place of purchased high voltage capacitors). This was done in both the Booster and Main Injector (MI) kickers with success. The capacitance of the Booster kickers is about 460 pF/m and is from the high voltage bus being approximately 27 mm from ground with ferrite and potting in between. The capacitance required for the MI Gap Clearing Kicker (MIGCK) is about twice as much per unit length due to the different aperture. This means some additional capacitive structure is required. This technique was used in the MI injection kickers.

Circuit simulations of the magnet were then done. Estimates of various parasitic capacitances were put in the model based on recent experience. The SPICE model of a previous kicker magnet section is shown in Figure 2. The current waveform of an existing pulser was used in the simulation. The magnet values used in the simulation are in Table 2 have been scaled for this kicker magnet. The total inductance per section is (La1+La2)*(1+K) = 58 nH, the capacitance is 23.2 pF and the impedance is then 50 ohms.

This inductance value is higher than the inductance estimated above and was done purposefully. Some method of tuning the impedance is required; there are too many variables in the construction of one magnet to the next. In the Booster extraction and MI injection kickers the spacing between the *capacitor* plates is changed to change the impedance. In that method the magnets are potted and the response is measured. If the capacitance is too low, the rubber is cut down. If the capacitance is too high, shims are added to the ground and more potting material is added. This does not effect the field strength of the magnet but does effect the rise time. This method is time consuming when building many magnets and can also compromises the integrity of the rubber in the high electric field region. The method that will be used for tuning the MIGCK magnets is to change the *magnetic* width of the gap by moving the return conductor to change the space between the supply and return conductors. This also keeps the field in the magnet the same and changes the rise time but does not compromise the high voltage regions of the rubber.

A variation in stray inductance of the capacitors (LC) was studied in SPICE, Figure 3. A value of up to 550 nH was not a severe problem. The simulation showed that 32 sections of magnet would just meet the 57 ns rise time requirements. (At the time the simulation was done it was 1% to 99% and had not yet been revised to 3% to 97%. It can be seen from the plot that the 3% to 97% rise time is about 48 ns). The design was changed to 28 sections *by making the magnet shorter* to provide for some margin in rise and fall time. Detailed mechanical drawings were then started. A prototype magnet would be built and tested to verify performance. Since the magnet is somewhat shorter, the total kick strength may fall short of the requirements. If there is

La1, La2, Lb1, Lb2	23.4 nH	RLa,RLb	2.5m Ohm
K(La2,Lb1)	0.24	LC	275 nH, 550 nH, 1100 nH
C	23.2 pF	RLC	200 Ohm
RPL	30 Ohm	CL	20 pF

Table 2, Spice Model Parameters

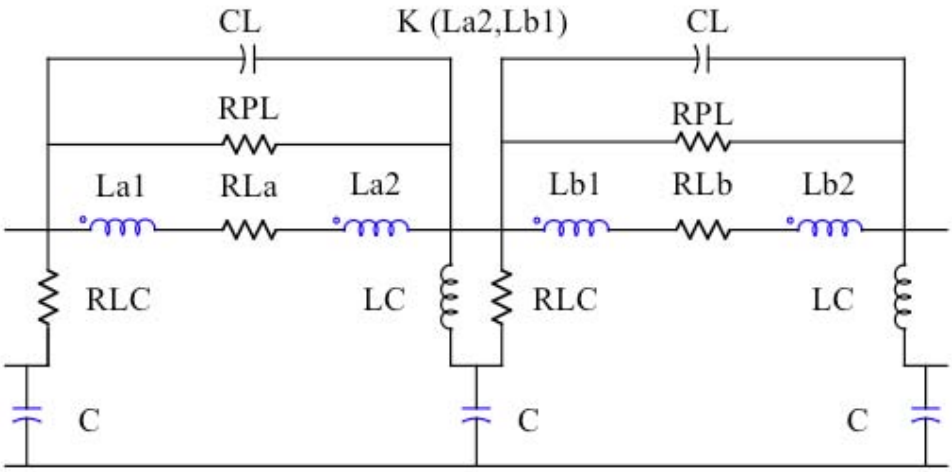

Figure 2, SPICE Magnet Model, 2 Sections

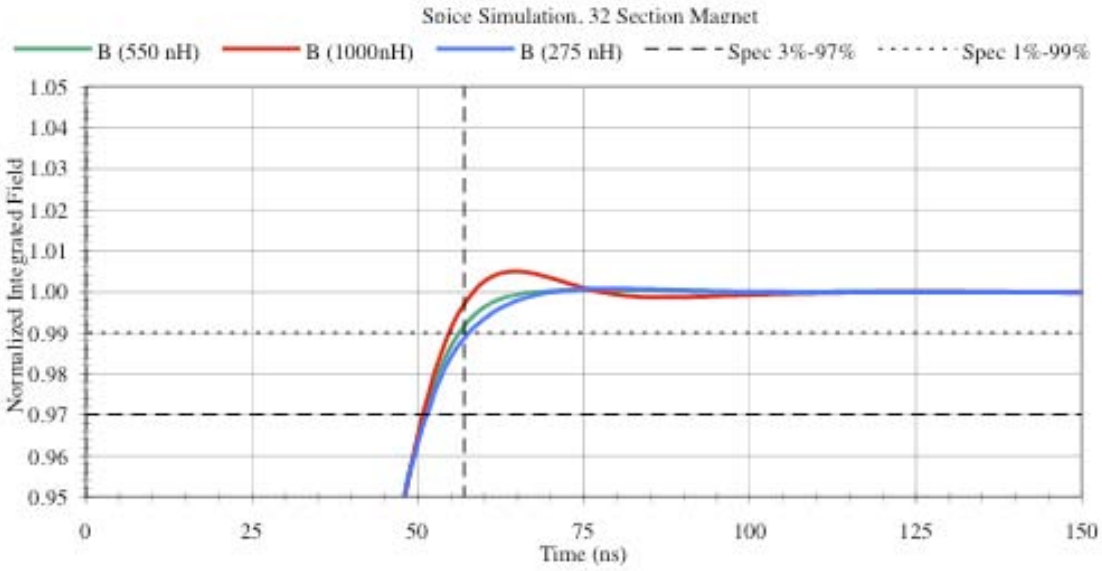

Figure 3, SPICE Simulation Plotting Total Integrated Field with different values of LC

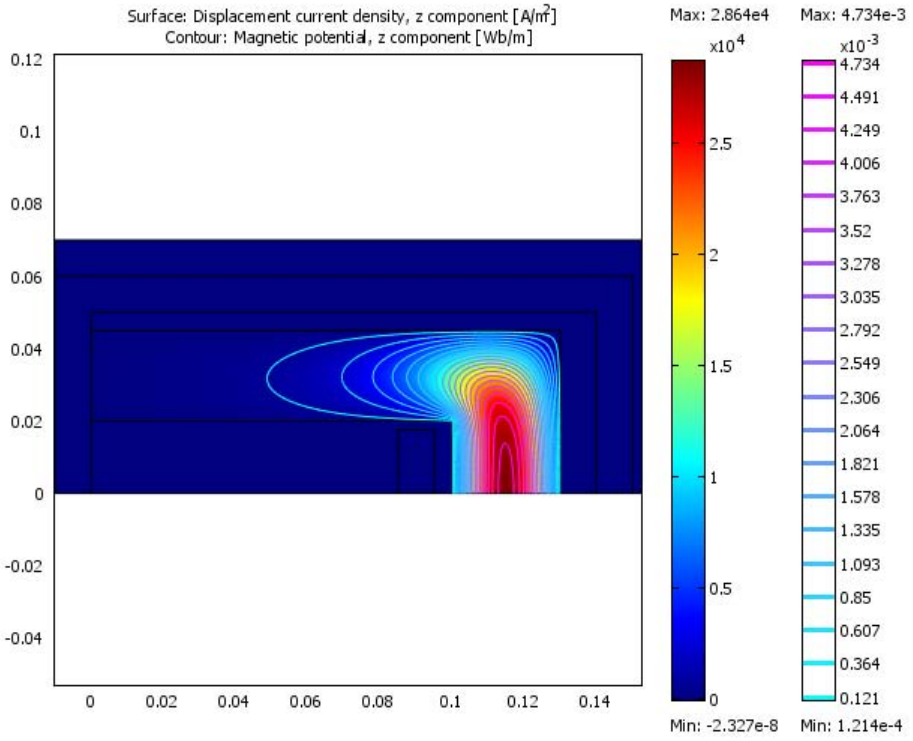

Figure 4a, Dimensional resonance effects in a simple ferrite C shaped kicker magnet. μ initial 1500, relative dielectric constant 15, ferrite width 2.5 cm, resonant frequency ~38 MHz

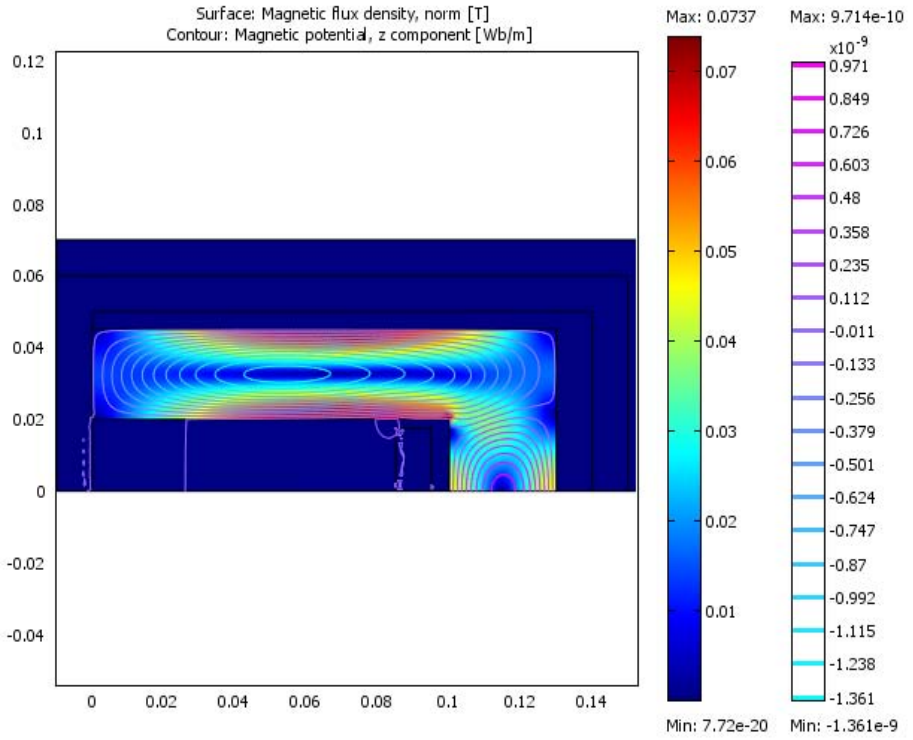

Figure 4b, Dimensional resonance effects in a simplified ferrite C shaped kicker magnet. μ initial 1500, relative dielectric constant 15, ferrite width 2.5 cm, resonant frequency ~46 MHz

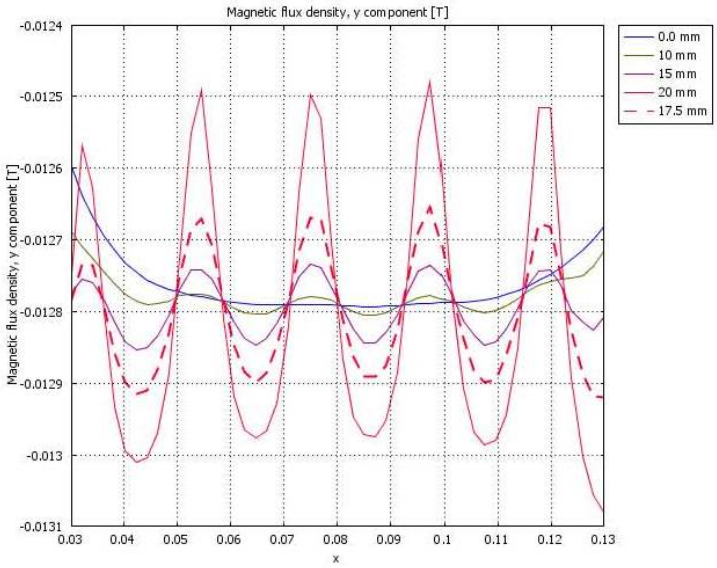

Figure 5, Effect of 5 mm spacing between ferrites 16.5 mm wide on field uniformity as a function of height above center line. The curvature near the ends are end effects in the model and the gap height from center line is 26 mm. The total integrated field at each position is equal.

sufficient margin in rise time, then the number of sections could be increased. Otherwise, the nominal current in the magnet would be increased to get the correct total strength

There was significant field modeling work done on the magnet using Comsol. Early modeling in 2D looked for dimensional resonance effect in the ferrite. This was thought to be a problem in some existing kicker magnets. The magnets apparent resonant behavior occurs at frequencies different than predicted by the simple LC-C resonance. The modeling showed there can be strong resonance effects in the 10's MHz frequency range with high permeability, low loss cores, Figure 4a, 4b. The first resonance did not strongly alter the field in the air gap and when realistic losses are added the effect is further reduced. The permeability also drops off with frequency, which again limits the effect. Still, the choice of ferrite width was made small to reduce the resonance by keeping the ferrite dimensions as small as reasonable without saturation issues.

The distance between sections, or equivalently the fill factor, has a strong effect on the magnet performance. There are three effects; local uniformity in field goes down with increased spacing (Figure 5), coupling between sections (KLa2Lb1) goes down with increasing spacing, and stray inductance of the capacitor (LC) goes down with increasing spacing. The last two are hard to unfold because they are measured in the same manner; the coupling between cells is equivalent to a decrease in the stray inductance of the capacitor lead. Modeling of the magnet was tried in 2D to estimate capacitor lead inductance but it was soon realized that a full 3D model was required and was not pursued further. The capacitor lead was also made to extend past one edge of the ferrite. This serves as a high frequency flux barrier which should reduce lead inductance. The flux path length is around the lead, forcing it on onse side through more air instead of the short path between ferrite blocks. The space between ferrite sections was chosen eventually based on electric field issues around the capacitor lead, but also without causing significant distortion to the integrated field or saturation problems.

The last two simulation issues that still needed to be resolved were the geometry to get the required capacitance and the resulting maximum electric field in the potting material. The initial simulation of the magnet was a simple 2D model to get the approximately correct electrode geometry. This showed that a rod in a groove could provide enough capacitance and have an electric field of less than 10 kV/mm with 27 kV on the magnet. The capacitance in this arrangement is also very tolerant of position errors. The 2D model was sufficient to produce drawings for fabrication of the required parts but a 3D model is required to perform the confirmation. The results of that model are discussed later. It was also planned to make minor corrections to the electrode based on measurement results before production was begun. The next section addresses the issue of the maximum electric field in the potting material.

Electric Field Stress

This magnet is intended to be potted with room temperature vulcanizing (RTV) silicon rubber. What is electric field stress level in the dielectric for long life? This is a critical question for both the magnet and system design. As mentioned earlier, the magnet had been shortened to allow for some margin in rise time. If it cannot be lengthened, the operating level of the magnet must be increased, which may then have lifetime implications.

There are several kicker magnets at Fermi with years of operating lifetime. The existing Main Injector injection kickers are fast rise time magnets with a good lifetime. These kickers have been running from October 1999 to May 2005 (Pbar main user) at about 1 Hz average, from May 2005 then to Jan 2006 (Numi) at about 2.5 Hz and from Jan 2006 to now (Slip Stacked Numi) at about 4.5 Hz average at about 25 kV on the magnet. There have been no failures on 3 magnets installed in the tunnel. A 2D electric field model was done and the maximum electric field is approximately 8 kV/mm. The stated dielectric strength for Sylgard 184 when cured in 0.125” thick samples, 60 Hz is 550 V/mil (21.6 kV/mm). In contrast, the Booster extraction kicker magnets at L-12 have a much higher failure rate of about 1 per year while operating at only 10% more pulses (Booster extraction to MI injection + MiniBoone). The maximum 2D field in the Booster kickers is more than 20 kV/mm, however the magnets do not fail where the 2D model shows a high stress. It is not clear what the primary cause of failure is, but the failures are at the end of the magnet. Some catastrophic failures are arc through from the high voltage bus to ground near the cable connection where the RTV has become brittle. Most failures are tracking problems where the grease used to make the termination has dried out and they can be fixed in place by cleaning and re-greasing the termination. The Booster kicker magnets also have a much higher residual radiation level (~100 mrem/hr) than MI-10 (~10 mrem/hr). The Booster kicker magnet and PFL failure rates have dropped recently since another magnet system was added and the voltage on the magnet dropped by 20%. The other potted kicker with long life is in pbar debuncher kickers. These kicker magnets use a ceramic capacitor to get the required capacitance and the peak electric field in the potting is only about 5 kV/mm.

Magnet Type	Nominal Magnet Voltage	Electric Field (Capacitor Region, 2D)	Electric Field (Peak, 2D)	Location of Peak Field
Booster Kicker	33 kV	4 kV/mm	20 kV/mm	Triple point between bus, potting and ferrite
MI Injection	25 kV	4 kV/mm	8 kV/mm	Around capacitance flag edge
Pbar Injection	25 kV	n/a	5 kV/mm	Around high voltage bus
MIGKC	27 kV	6 kV/mm	10 kV/mm	Around edge of electrode

Table 3, Simulation results, electric field stress in kicker magnets

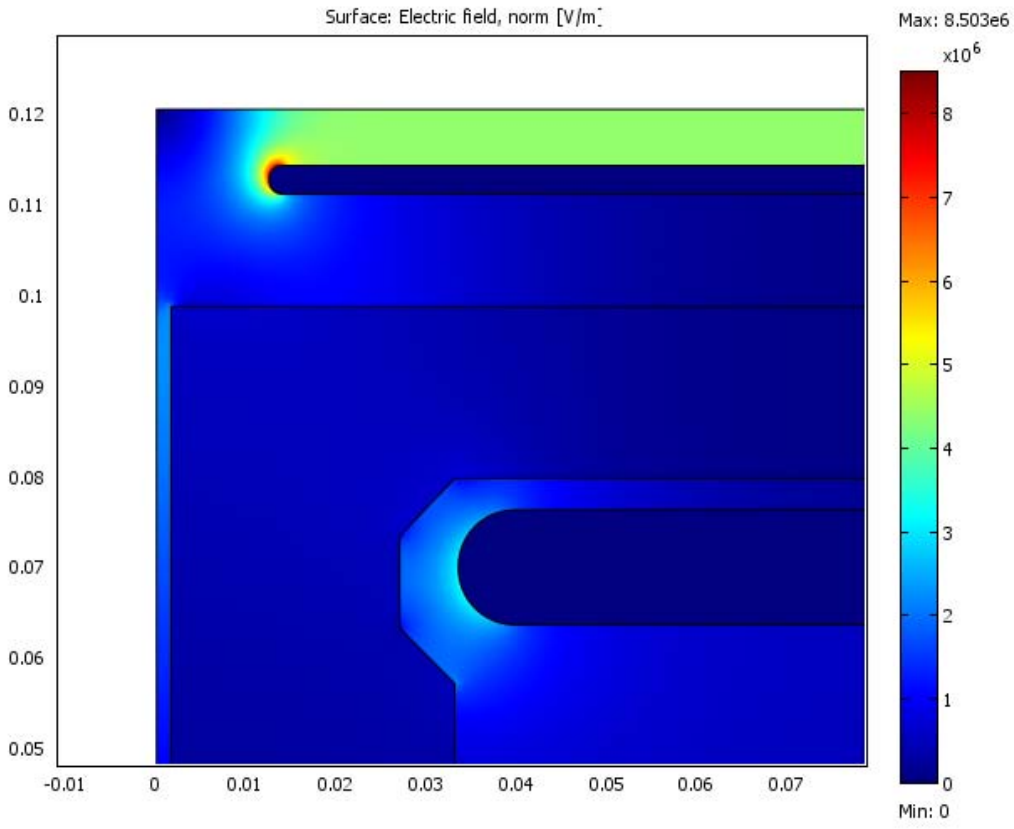

Figure 6, MI -10 Kicker Magnet Electric Field, 27.5 kV Bus Voltage

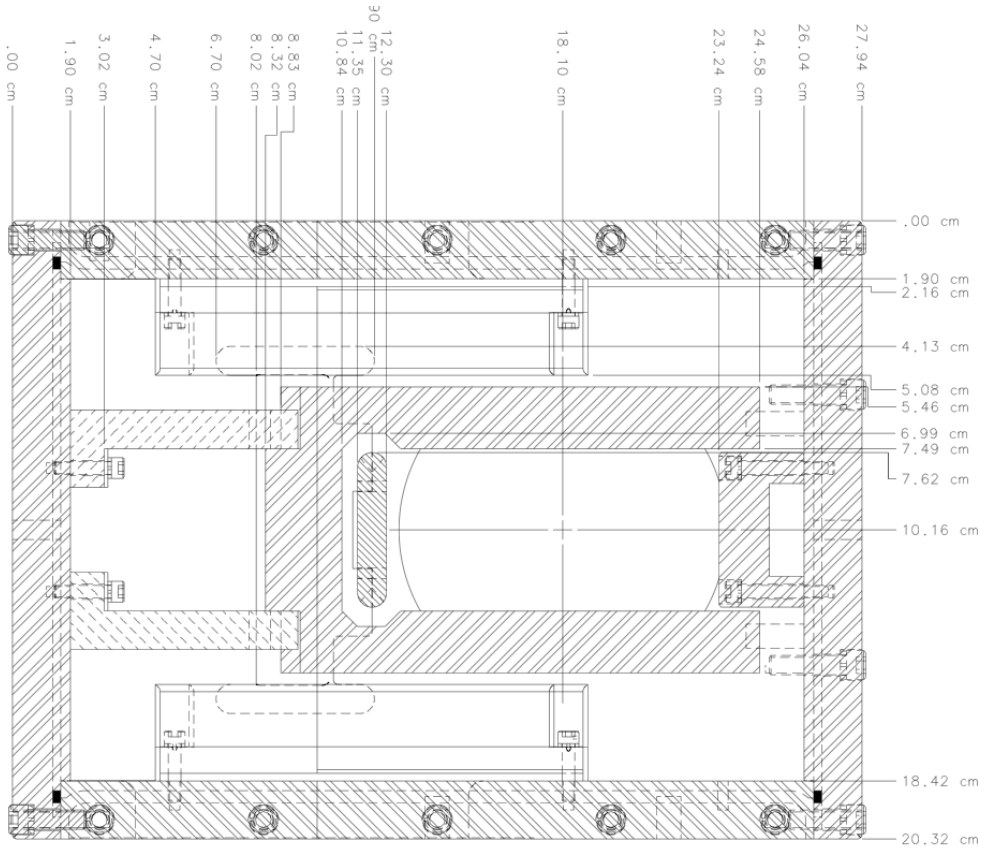

Figure 8, Current magnet assembly model

3 Prototype Magnet Measurements

The plan for the prototype magnet was to order most of the parts, then assemble and test. The longest lead time and most expensive of any of the components of the magnet is the ferrite. To allow for a cost effective comparison of ferrite materials, only half the high voltage capacitor plates were attached to the high voltage bus. This meant that only half the amount of ferrite for a full magnet would be required and four different types of ferrite could be tested. After the ferrite tests were complete, the full complement of capacitors could be installed and the remaining ferrite of the preferred type could ordered. Then magnet tests could be completed.

The capacitance was measured and modeled in 3D with the prototype magnet in various configurations. The model was of a single section with boundary conditions to match a continuous magnet. The capacitance of the high voltage bus alone (without capacitors attached) was measured. This verified the geometry of the model. The magnet was also measured with the capacitors attached, but with and without ferrite. This verified the ferrite dielectric constant in the model. It also showed that 20% changes in the ferrite dielectric constant would not make substantial changes in the capacitance. The magnet was then filled with an insulating oil, FC-77, with a relative dielectric constant of 1.86. Finally, a vacuum chamber was inserted into the magnet. This chamber was coated with graphite to get a resistance of 2500 Ohms, approximately the resistance in the actual tube. The chamber and coating are known to have a substantial effect of the capacitance of both the Booster and MI kickers.

The capacitance for each section from the model and from measurement are shown in Table 5. The final agreement of measurement to model would be exact with an additional 0.7 pF at for each cell, which is still a 3% effect. The ratio of bus capacitance with and without FC-77 is 1.83 in the measurements vs. 1.85 in the simulation, which shows good agreement. The error between model and measurement may simply be mechanical tolerance issues on the capacitor spacing. The tolerance on the capacitor rod and on the channel width was ±0.005". If the rod was oversize at the extreme and the channel undersize, that would account for the observed error. These tolerances have been tightened to ±0.003". Modeling of the coated beam tube was not possible given the resistivity and frequency of interest. However, the measured change in capacitance can be use. The final design of the capacitor can now be completed, the model have been proven and the chamber capacitance having been determined.

Frequency / Total C	100 kHz Meas.	400 kHz Meas.	1 MHz Meas.	Model, DC (Total)	Model, DC (Cell)
Cend (w/test connections) in air	21.1 pF ± 0.5 pF	21.2 pF ± 0.5 pF	21.2 pF ± 0.5 pF	n/a	n/a
Cend (w/test connections) in FC-77	30.2 pF ± 0.5 pF	30.2 pF ± 0.5 pF	30.3 pF ± 0.5 pF	n/a	n/a
Chv bus (-ends) *	33.7 pF	33.6 pF	33.6 pF	34.1 pF	0.93 pF
Chv bus + 14 flags in air (-ends) #	331.6 pF ± 1.5 pF	331.8 pF ± 1.5 pF	330.3 pF ± 1.5 pF	320.9 pF	21.70 pF
Chv bus + 14 flags in FC-77 (-ends) #	609.1 pF	609.0 pF	610.9 pF	594.0 pF	40.16 pF
Chv bus + 14 flags w/ ferrite in air (-ends)	350.4 pF	346.7 pF	348.3 pF	334.9 pF	22.72 pF
Chv bus + 14 flags w/ ferrite + coated beam tube in air (-ends)	399.3 pF	389.2 pF	388.0 pF	n/a	n/a

Table 4, Comparison of measured and simulated capacitance. Notes: * Total bus length is 33", so number of 0.9" sections is 36.7, # 16.5" bus + 14 flag sections, error estimates are done from having 2 measurements, mean is listed and error is difference from mean and two measurements

Similar modeling was done for inductance, in 2D and 3D. The 3D model has a difficult time converging at frequencies above 100 kHz (given the constraint of computer memory). There are strong effects on the calculation result depending on the way the mesh is made because the skin depth is comparable to the mesh size. There is still substantial agreement at 100 kHz.

The end effects on inductance were not modeled, but they were measured. The inductance was measured by placing a short in place of successive capacitors for the first 10 capacitors (9 ferrites). The inductance of the first section is 171 nH, 3.2 times the middle section inductance and the inductance of the second section is 82 nH, 1.5 times the middle section inductance. By the third section, the inductance is only 15% higher and the fourth section is about 2% higher. The extra inductance of the first sections does not include input connection or capacitor lead inductance. The inductance of the capacitor lead (LC in SPICE) was measured to be ~ 28 nH (two leads of 56 nH each). The inductance from the input to the first section is ~ 95 nH in the AC test setup and will increase to ~160 nH when the high voltage connection is used.

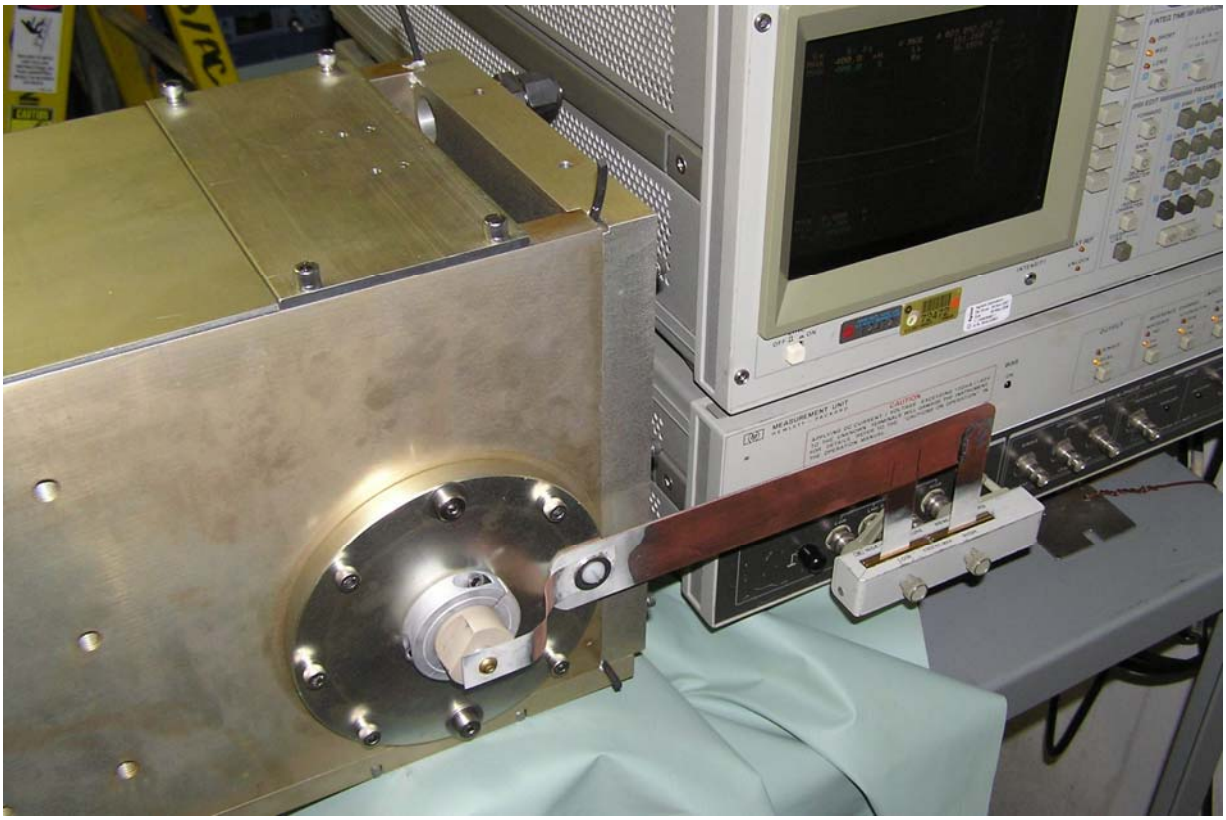

Figure 9, AC Capacitance and Inductance Measurements

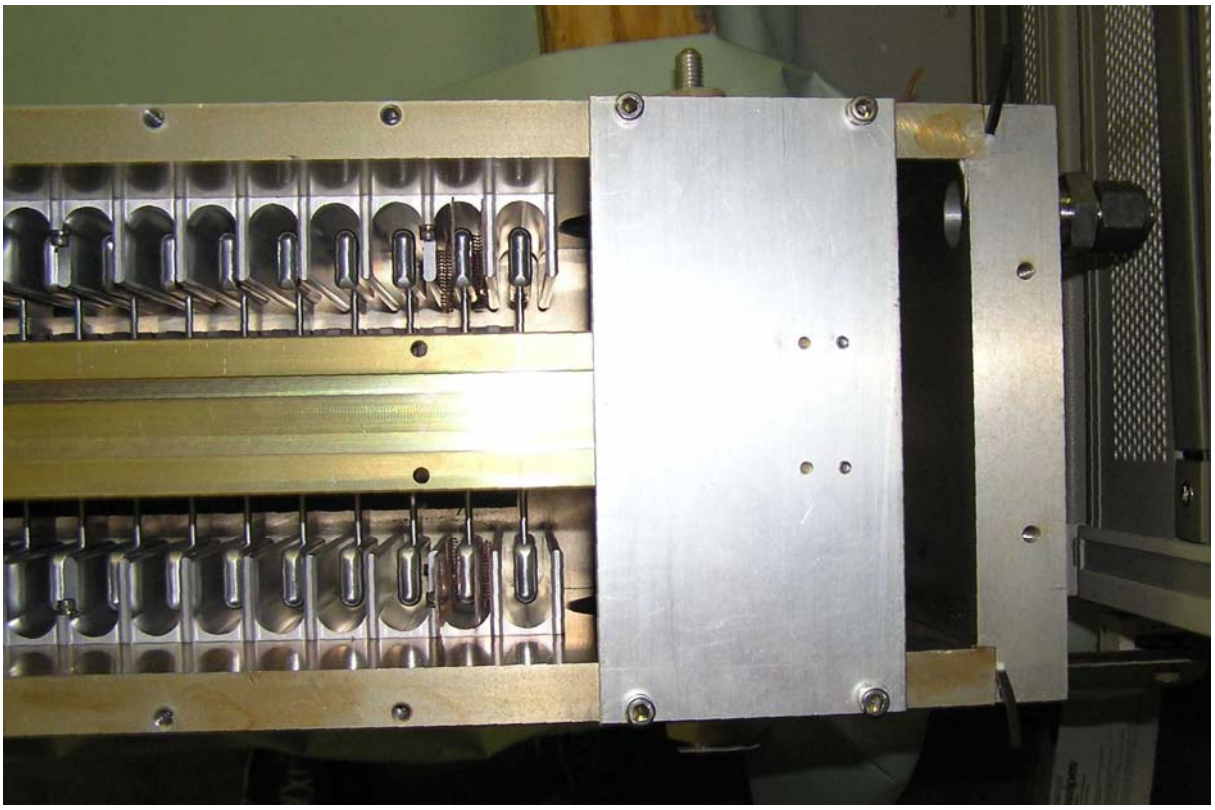

Figure 10, Top View with Ground Removed, Showing Capacitor Structure.

Frequency / Total C	100 kHz	400 kHz	1 MHz
L/section Measured (4.50" Gap)	55.3 nH ±0.5 nH	54.4 nH ±0.5 nH	54.3 nH ±0.5 nH
L/section Calculated * (4.50" Gap)	54.6 nH	n/a	n/a

Table 5, Comparison of measured and simulated inductance. Notes:* Inductance was modeled for 4.47" Gap, then scaled by 4.50"/4.47"

After the capacitance and inductance were measured with the C2010 material, impedance measurements were done with the magnet resistively terminated at the midpoint (after the last ferrite) for all four ferrites. The ferrites chosen for use in test are CMD5005 (μ, initial=1500) and C2010 (μ, initial=350) from Ceramic Magnetics, G4 (μ, initial=400) and CMD10 (μ, initial=450) from National Magnetics. The resistor was changed until the phase response gave the flattest curve (Figure 11); this gives the best pulse response. The best termination value was 47.3 Ohms for CMD10, 48.5 Ohms for CMD5005, 46.6 Ohms for C2010 and 47.0 Ohms for G4. This is in general agreement with the relative permeability These ferrites were chosen for their relatively high permeability and high frequency response. Values of permeability less than 100 give poor field uniformity in the air gap. All the ferrites are NiZn but the CMD10 formulation has a higher saturation flux.

Next, a low loss, 50 Ohm cable approximately 80 ns long was connected to the magnet from a fast, low voltage pulse generator. Custom, low impedance (10 kOhm) voltage probes were installed in the magnet so that the input and end point voltage could be measured. These voltages were then saved to disk and imported to a spreadsheet. The offset of raw data for each channel was found and subtracted from the signal by looking at the null signal just before the pulse arrived at the magnet. Then, the gain of one of the channels was adjusted until the input and endpoint signal had the same average value during the flattop (after all reflections had died down). Finally, the difference of input to endpoint was found and summed (integrated) over the pulse. The resulting signal is directly proportional to the total flux in the magnet. Since the magnet has a gapped core, we can safely assume that the majority of the flux is in the air gap. Because of the structure of the magnet, we can also assume most of the flux is normal to the particle trajectory. This technique of measuring the total flux in the magnet has been used for some time at Fermi and has been found to be an accurate method when compared to B-dot coil techniques or even actual measurements with beam. This same process was repeated for all the ferrite materials.

Looking at the results in Figure 12 there is not a large variation in response. What is actually critical in this application is sufficient loss in the ferrite to damp oscillations caused by the coupling between sections and capacitor lead inductances. It is also seen that the materials with a high permeability have a slower response. This is a known characteristic of ferrites. The frequency for maximal losses in a ferrite (therefore maximal change in permeability, and hence maximal useful frequency) is given by the following formula (from Snoek, assuming domain rotation is the source of initial relative permeability)

$$f_{max} = \frac{\gamma M_{sat}}{3\pi(\mu_{r,initial} - 1)}$$ where γ is is the gyromagnetic ration, 2.2 10^5 (rad/s)/(A/m)

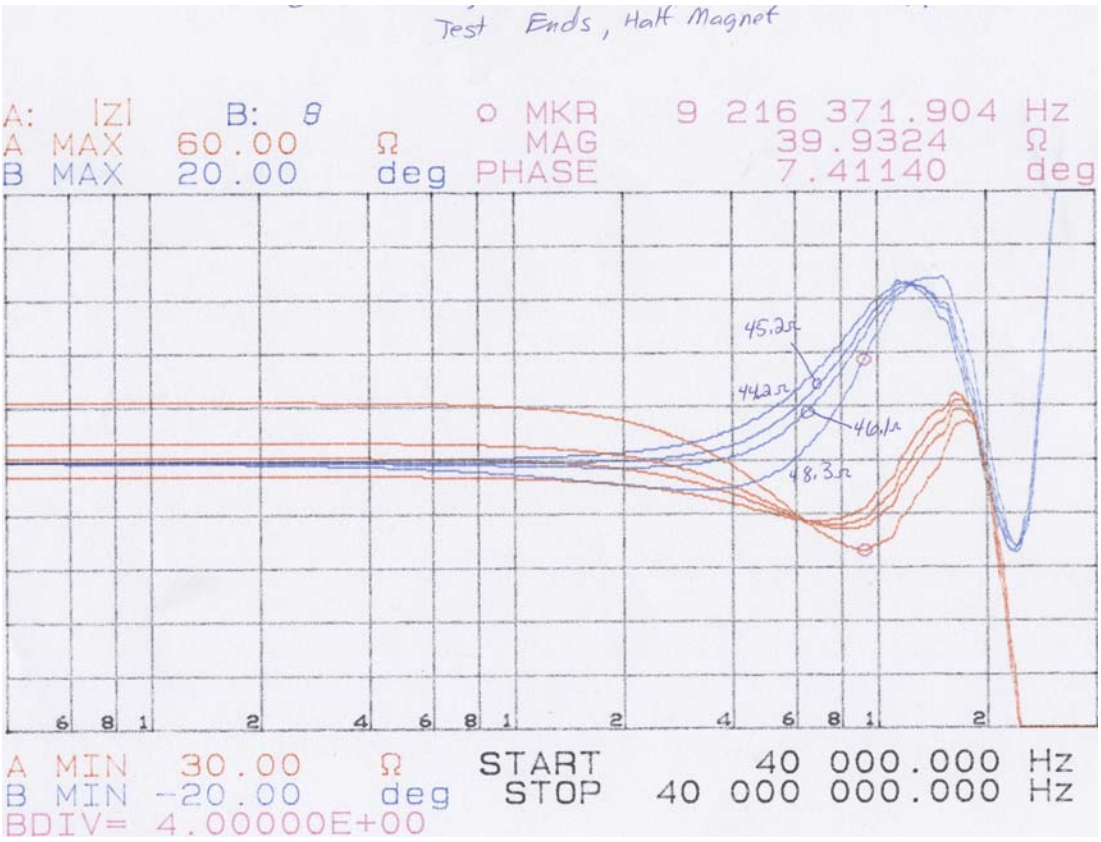

Figure 11, Magnitude and Angle vs. Termination Resistance for C2010 Prototype

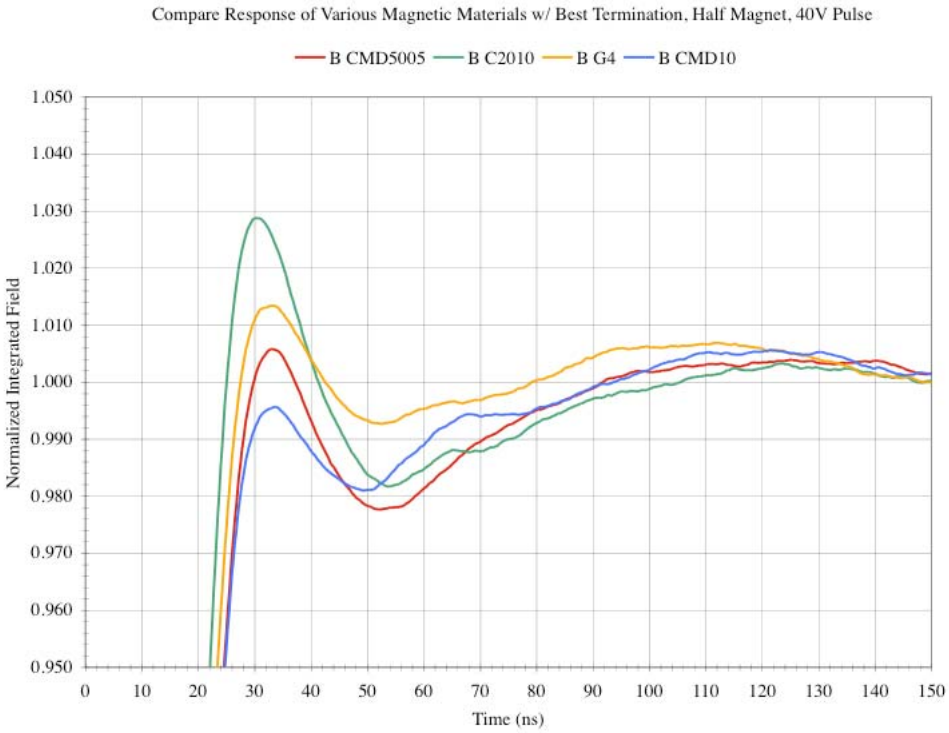

Figure 12, Low Level Pulse Measurements for Half Filled Magnet

The CMD10 material has a higher saturation magnetization and coupled with its lower initial μ it might have provided a faster response. However, the test shows that in our application the G4 material will be best. It has a slightly slower rise time than the C2010, but is also more lossy and therefore does a better job at damping out the internal oscillations in the magnet.

Magnet pulse measurements were then done with all sections loaded with ferrite. Since we did not have sufficient time available, the magnet was filled with 50% G4 and 50% C2010. These two ferrites are very close in properties and should yield good representative results. The magnet was run in air at approximately 4 kV (8 kV charge on the PFL). At this voltage high bandwidth (300 MHZ) 5 kV probes could be used to directly measure the voltage on the high voltage bus. Measurements were taken at a low repetition rate (1 pps) and were averaged in the scope over 1000 samples. This data was saved and then the probes were reversed on the magnet. This will compensate for any probe gain difference and was done to avoid using an arbitrary relative gain as was done for the low level measurements. The offset for each probe was removed by looking at the level before the pulse came and subtracting that from the amplitude. The same technique used in low level measurements was used to calculate the integrated field. The resulting rise time is shown in Figure 15 and fall time in Figure 16.

The requirements are met on the rise and fall time and almost on the flatness. Fig 17 shows the voltage on the input and output of the magnet during the rise time. It can be seen that there is a dip in the input voltage. Typically, capacitance is added to the magnet output to prevent overshoot, however this dip is due to excessive capacitance at the output. Some additional inserts were used to reduce inductance from input/output to the first/last cell. These also added more capacitance but the existing capacitance was not changed. The end capacitance will be corrected to remove the dip by using a SPICE simulation of the magnet to determine the correct input/output capacitance.

The operating voltage of the magnet can now checked. Given the measured inductance of the magnet (1.77 μH), and the gap width (11.4 cm) we can determined the required current from

$$B \quad A = L \quad I \Rightarrow B \quad l = \frac{L \quad I}{w}$$

where B is flux magnet, ~ flux in the gap
A is area normal to flux, w x ~l
w is the distance between high voltage and return bus
l is the length of the magnet
L is magnet inductance
I is magnet current

The required kick angle is then

$$\theta_B = \frac{B \quad l}{B_\rho} = \frac{L \quad I}{w \quad B_\rho} \text{ and } \theta_E = \frac{I \quad Z_0}{w}$$

where B l is the integrated magnetic field normal to the beam
B_ρ is the rigidity, which is 29.65 for 8 GeV/c^2 proton kinetic energy
Z_0 is the load resistance, 50 Ohms in this case
θ_B, θ_E are the magnetic field deflection and the electric field deflection

We will be installing the magnet so that the electric field kick and magnetic field kick add. With the 6 magnets for MI Gap Clearing we get a nominal current of 510 A so a magnet voltage of

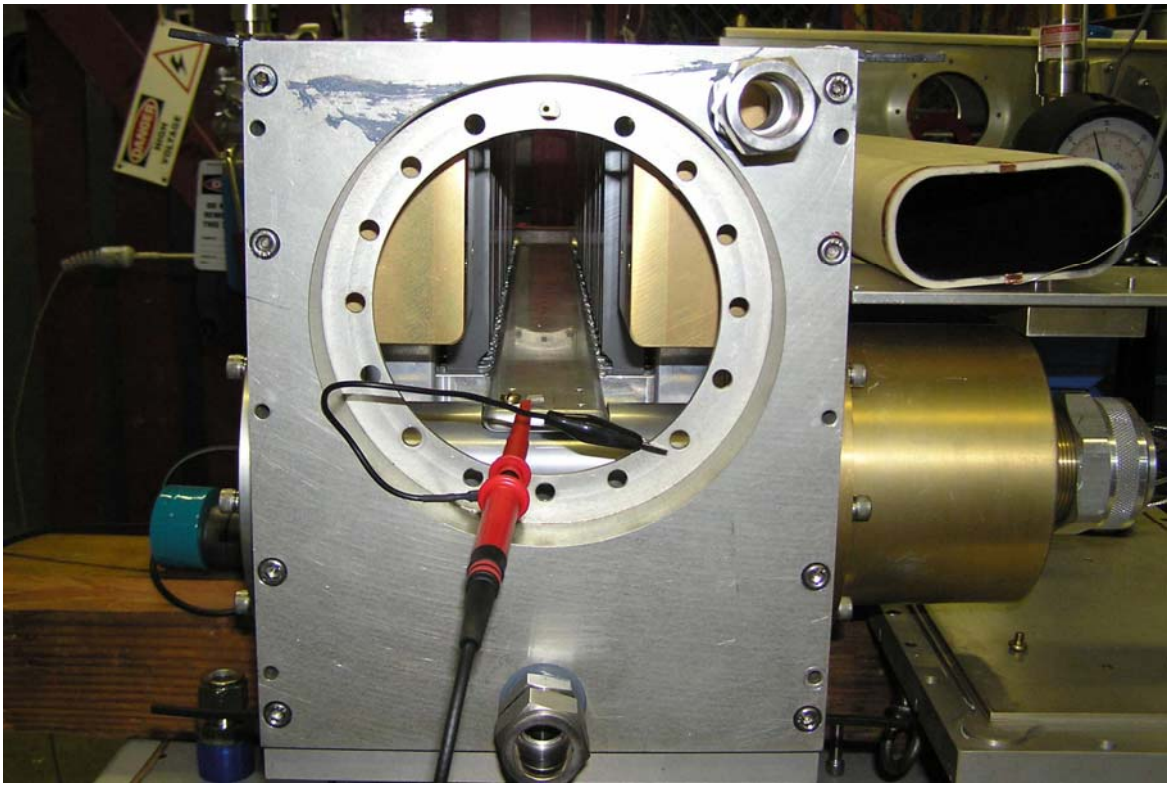

Figure 13, High voltage measurement, ceramic chamber used during testing is shown at right.

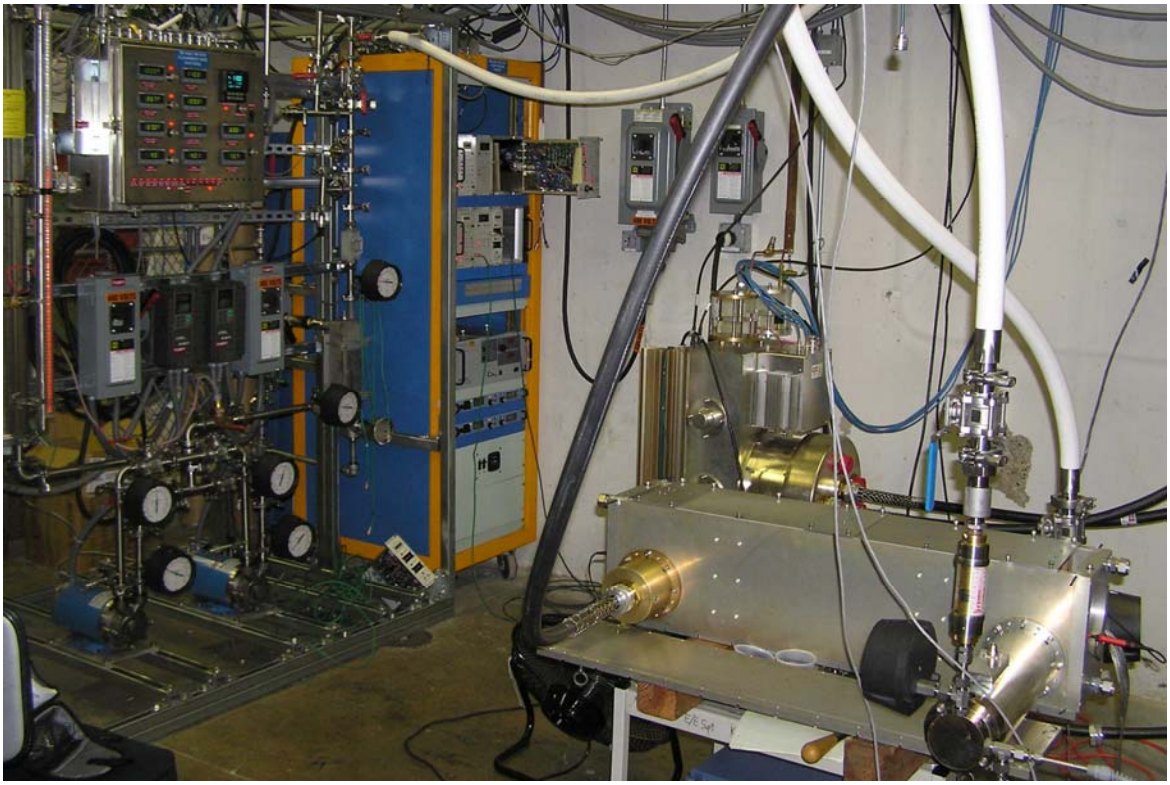

Figure 14, Test area showing magnet, pulser and controls

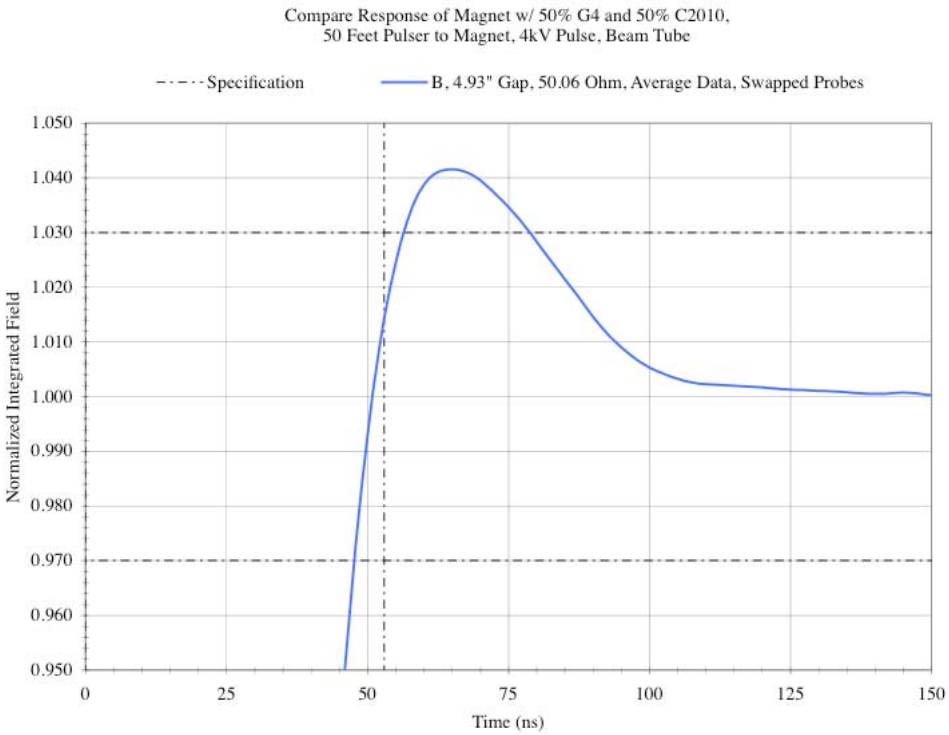

Figure 15, Calculated Magnet Field based on Terminal Voltages, Showing Rise Time Detail

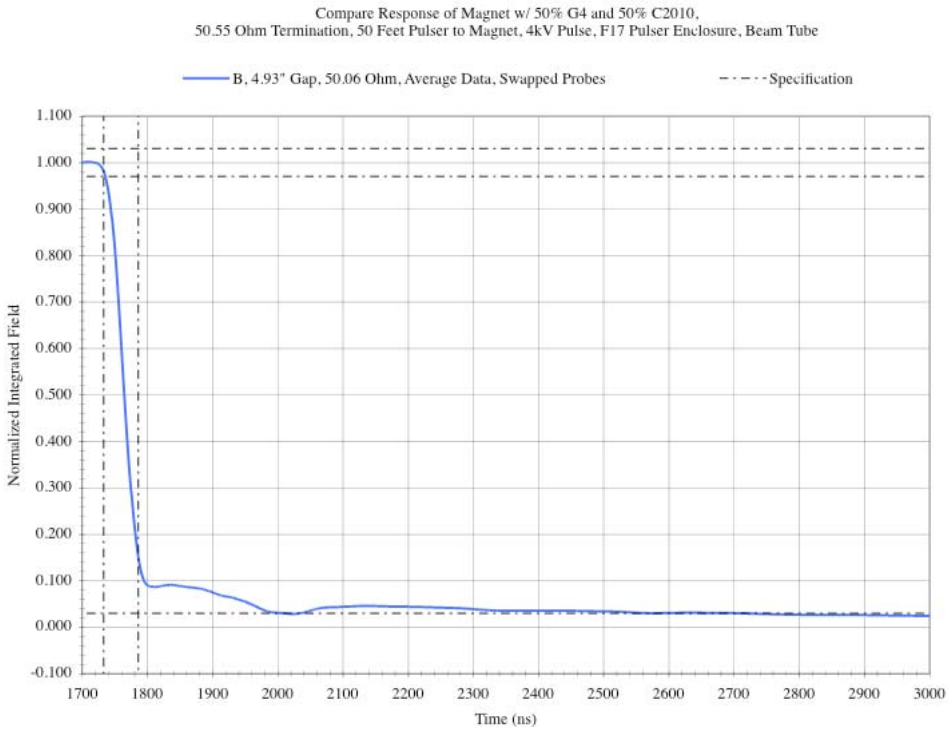

Figure 16, Calculated Magnet Field based on Terminal Voltages, Showing Fall Time

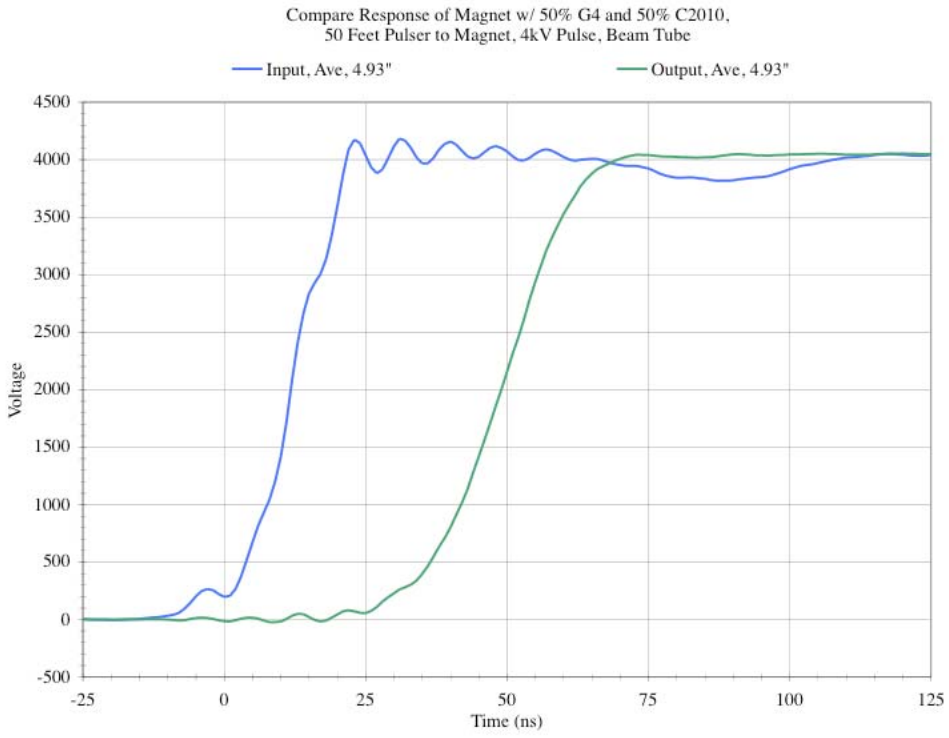

Figure 17, Measured Input and Output Terminal Voltages

25.5 kV, or a PFL charge of 51 kV. Typically we allow for a 10% tuning range so the maximum voltage will be 56 kV. For RR Gap Clearing the nominal voltage would be 22 kV on the magnet, 44 kV PFL charge, or 48.5 kV including 10% tuning range.

Conclusions

The magnet can meet all the specifications and measurements and field models have been verified. A SPICE model still has to be completed so that simulation of the magnet can choose the correct end capacitance to reduce overshoot at the rising edge.

The MI Gap clearing maximum voltage is above where we would like to operate for long term reliability of the PFL. We would limit the power supply to 55 kV and have only 8% tuning range. At this point there are a variety of choices on how to handle the tuning range. But, the question remains regarding the maximum electric field stress at which to run the dielectric. At 27.5 kV on the magnet (maximum operating), the peak stress in the magnet will be 10 kV/mm. This could be reduced by adding another magnet and power supply IF this stress level is to high. Another option would be to change the magnet substantially, e.g. by changing the section length, so that the electric field can be reduced. There are other options one could explore but none answer the question of stress level. The stress level for RR Gap Clearing at nominal voltage is ~8 kV/mm, the same as the 2D model of the MI injection kicker.

A pre-production magnet is being built. Ferrite for all the magnets has been ordered. The new capacitor still requires some simulation work to get the correct capacitance. This design will then be installed into the pre-production magnet.